HHS Public Access

Author manuscript

Bone. Author manuscript; available in PMC 2016 March 01.

Published in final edited form as:

Bone. 2015 March ; 72: 92–100. doi:10.1016/j.bone.2014.11.018.

Loss of the PGE2 Receptor EP1 enhances bone acquisition, which protects against age and ovariectomy-induced impairments in bone strength

Minjie Zhang[1,2], **Marina Feigenson**[1], **Tzong-jen Sheu**[1], **Hani A. Awad**[1,3], **Edward M. Schwarz**[1], **Jennifer H. Jonason**[1], **Alayna E. Loiselle**[1], and **Regis J. O'Keefe**[1,4,*]

[1]Center for Musculoskeletal Research, Department of Orthopaedics & Rehabilitation, University of Rochester Medical Center, Rochester, New York 14642

[2]Shenzhen Institutes of Advanced Technology Chinese Academy of Sciences, Shenzhen, China

[3]Department of Biomedical Engineering, University of Rochester, Rochester, NY, 14627

[4]Department of Orthopaedic Surgery, Washington University in St. Louis School of Medicine, St. Louis, Missouri 63110

Abstract

PGE2 exerts anabolic and catabolic effects on bone through the discrete actions of four prostanoid receptors (EP1-4). We have previously demonstrated that loss EP1 accelerates fracture repair by enhancing bone formation. In the present study we defined the role of EP1 in bone maintenance and homeostasis during aging and in response to ovariectomy. The femur and L4 vertebrae of wild type (WT) and *EP1*$^{-/-}$ mice were examined at 2-months, 6-months, and 1-year of age, and in WT and *EP1*$^{-/-}$ mice following ovariectomy (OVX) or sham surgery. Bone volume fraction, trabecular architecture and mechanical properties were maintained during aging in *EP1*$^{-/-}$ mice to a greater degree than age-matched WT mice. Moreover, significant increases in bone formation rate (BFR) (+60%) and mineral apposition rate (MAR) (+50%) were observed in *EP1*$^{-/-}$, relative to WT, while no change in osteoclast number and osteoclast surface were observed. Following OVX, loss of *EP1* was protective against bone loss in both femur and L4 vertebrae, with increased bone volume/total volume (BV/TV) (+32% in femur) and max load at failure (+10% in femur) relative to WT OVX, likely resulting from the increased bone formation rate that was observed in these mice. Taken together these studies identify inhibition of EP1 as a potential therapeutic approach to suppress bone loss in aged or post-menopausal patients.

*Corresponding Author: Regis J. O'Keefe, Department of Orthopaedic Surgery, Washington University in St. Louis School of Medicine, Campus Box 8233, 660 South Euclid Ave., St. Louis, MO 63110-1093, okeefer@wudosis.wustl.edu.

All authors state that they have no conflicts of interest.

Authors' roles: Study design: MZ, MF, JHJ, AEL, RJO; Data collection: MZ, MF, TJS; Data analysis: MZ, MF, TJS; Data interpretation: MZ, MF, HAA, EMS, JHJ, AEL, RJO Drafting manuscript: MZ, MF, TJS; Revising manuscript content: HAA, EMS, AEL, JHJ, RJO; Approving final version of manuscript: MZ, MF, TJS, HAA, EMS, JHJ, AEL, RJO; MZ, MF and RJO take responsibility for the integrity of the data analysis.

Keywords

EP1; PGE2; ovariectomy; age-related bone loss; mouse model; bone homeostasis

Introduction

Prostaglandin E2 (PGE2) is produced by arachidonic acid metabolism and is synthesized via the cyclooxygenase (COX) and prostaglandin synthase pathways. COX-2/PGE2 signaling mediates both physiological and pathological effects in a vast array of tissue types, including bone (1–4). The broad effects of PGE2 are attributed to the four prostanoid receptors which bind PGE2: EP1, EP2, EP3 and EP4. These four receptors differ in tissue distribution, ligand binding affinity and activation of downstream signaling pathways (1,3,5). EP2, EP3 and EP4 modulate cAMP levels (3,5). EP2 and EP4 activation stimulates the production of cAMP through $G\alpha_s$. In contrast, EP3 activation results in decreased cAMP levels through $G\alpha_i$, $G\alpha_q$, or $G\alpha_s$, depending on the EP3 isoform. Less is known about the EP1 receptor. While the EP1 receptor is involved in regulating intracellular calcium levels, the G protein to which it couples remains to be identified.

In bone, PGE2 exerts both anabolic and catabolic effects (6–9). Administration of PGE2 to mice lacking each of the four prostanoid receptors identified EP4 as the primary mediator of PGE2-induced bone formation (10). While the role of EP1 in osteoblastic differentiation and bone metabolism is not as well defined, selective EP1 agonists have been shown to stimulate the proliferation of osteoblast progenitors, but impair osteoblastic differentiation (11). Consistent with these findings, we previously demonstrated that loss of EP1 accelerates osteoblastic differentiation and fracture repair (12). Although there is evidence supporting a role for PGE2/EP1 signaling in osteoblastic differentiation and bone regeneration, the effects of EP1 receptor signaling on bone homeostasis during two critical phases, growth and aging, is poorly understood. EP1 has been implicated in other aging-related pathologies including neurodegenerative disease (13) and hemin-mediated neurotoxicity (14). In the present study we examined the hypothesis that EP1 acts as a negative regulator of bone formation and skeletal growth, while loss of EP1 promotes maintenance of bone during aging. We report that *EP1*$^{-/-}$ mice have increased bone mineral density and stronger cortical and trabecular bone biomechanical properties. The trabecular bone of the *EP1*$^{-/-}$ mice is also resistant to and protective against aging-induced ovariectomy-induced bone loss. The altered bone properties of the *EP1*$^{-/-}$ mice result mainly from an increased bone formation rate. *In vitro* studies confirmed that the EP1 receptor acts to inhibit bone marrow osteoprogenitor cell differentiation and mineralization.

Methods

Experimental Animals

All animal studies were conducted with the approval of the University Committee on Animal Resources at the University of Rochester. Wild type C57BL/6J (WT) mice were purchased from Jackson Laboratories (Bar Harbor, ME) at 4-weeks of age. *EP1*$^{-/-}$ (KO) mice (15) are on a C57Bl/6J genetic background and were generously provided Dr. Matthew

Breyer (Vanderbilt University). Female mice were used for ovariectomy experiments, while male mice were used for aging experiments.

Histology and Histomorphometric Analysis

Femurs were collected from *EP1*$^{-/-}$ and WT mice at 2-months, 6-months, 1-year of age, or 8-weeks after OVX or sham surgery. Specimens were fixed in 10% neutral buffered formalin, decalcified for 21 days in 10% EDTA (pH 7.2), processed and embedded in paraffin. Three-micron sections were taken from three different levels (30μm lateral to the mid-shaft of the femur, mid-shaft of the femur, and 30μm medial to the femur mid-shaft), and stained for TRAP^{+} osteoclasts; sections were counterstained with Methyl green. At least five specimens per genotype per age were used for histomorphometric and histological analyses.

Micro-Computed Tomography (μCT)

Femurs and vertebrae were harvested and scanned at 10.5μM resolution using a Scanco VivaCT 40 (Scanco Medical AG). Trabecular Bone volume fraction bone volume (BV)/total volume (TV), number (Tb.N.), thickness (Tb.Th), and spacing (Tb.Sp) were measured in the distal metaphyseal region of the femur and the trabecular region of the L4 vertebrae. The femur trabecular bone region of interest (ROI) began 210 microns proximal to the last remnant of growth plate interrupting the trabecular space, and spanned 1060.5 microns proximally (101 10.5μm slices). Cortical BMD, polar moment of inertia (pMOI), area (Ct. Ar) and thickness (Ct. Th) were measured in the mid-diaphyseal region of the femur.

Biomechanical Testing

3-point Bending—Mechanical properties were assessed by three-point bending as we have previously described (16). Briefly, femurs were cleaned of soft tissue and mounted on two supports spaced 8mm apart on an Instron 8800 device (Instron). The femurs were loaded at a displacement rate of 0.10 mm/sec with data points recorded every 0.01 sec by Bluehill software (Instron). The maximum load at failure, energy to max, and stiffness were calculated from force versus deformation data.

Compression

The L4 vertebral body was tested in compression with loads applied along the craniocaudal axis using an Instron 8800 device at a rate of 3 mm/min. Load displacement data were captured using Bluehill software. The ultimate load, yield load, stiffness, ultimate stress, yield stress and young's modulus were determined.

Calcein Labeling Analysis

Two-month old mice, or OVX mice were given two doses of calcein (25 mg/kg; Sigma) seven days apart and were sacrificed 7 days after the last injection. Calcein labeled tissues were isolated from the calvaria and tibia, fixed in ethanol and embedded in OCT media for frozen sectioning. Tibiae were sectioned longitudinally through the medial bone; the intersection of the anterior cruciate ligament and the posterior cruciate ligament was used as the anatomical maker to signify the middle of the tibia. Calvaria were sectioned coronally

through the parietal bones into 5-micron sections and examined by fluorescent microscopy. The following parameters were examined and calculated: single and double labeled surface (sLS, dLS, mm), mineralizing surface (MS = dLS+1/2sLS, mm), mineral apposition rate (MAR = distance between calcein labels/7 days, μm/day), bone surface (BS, mm), and bone formation rate (BFR = [MS × MAR]/BS × 365/1000, mm/year).

Ovariectomy

Ovariectomy was performed in 4-month-old *EP1*$^{-/-}$ and WT female mice. Each ovary was removed from the abdominal cavity onto an aseptic field and disconnected at the junction of the oviduct and the uterine body. Mice were sacrificed eight weeks after ovariectomy. Serum estradiol levels were examined using a 17-β-estradiol enzyme immunoassay kit (Assay Designs, Ann Harbour, MI).

EP1 antagonist studies

Isolated bone marrow stromal cells were seeded as 2×10^6 cells per well of a 12-well plate. Cells were cultured in basal medium (α-MEM, 10% FBS, 1% Penn-Strep) for 5 days until cells were ~80% confluent; cells were then cultured in osteogenic media (α-MEM, 10% FBS, 1% Penn-Strep, 10mM beta-glycerophosphate (J. T. Baker) and 50 μg/ml ascorbic acid (Sigma) with either vehicle (DMSO) or 10 μM SC-19220 (EP1 antagonist) for five days. Media was changed every other day, with addition of fresh SC-19220 or vehicle. Cells were fixed with 10% formalin and stained with alkaline phosphatase. Alkaline phosphatase staining intensity was quantified from triplicate samples per group at an absorbance of 520nm, and normalized to staining in control cells.

Statistical analyses

Results are shown as the mean ± SEM. Statistical significance was identified by Student's t-tests or two-way ANOVA followed by Dunnett's test. p-values less than 0.05 were considered significant.

Results

Loss of EP1 increases bone volume fraction and bone strength

Based on the accelerated fracture healing phenotype of *EP1*$^{-/-}$ mice and the enhanced osteoblastic differentiation observed in *EP1*$^{-/-}$ mesenchymal progenitors, relative to WT (17), we sought to determine the effects of *EP1* deletion on bone homeostasis. We examined the baseline bone phenotype in WT and *EP1*$^{-/-}$ mice between 2 and 12 months of age by microCT. Reconstruction of microCT data collected from the distal metaphyseal region of the femur showed progressive loss of trabecular bone as a function of age in WT mice; in contrast, bone loss is delayed and is less severe in *EP1*$^{-/-}$ mice. No changes in trabecular parameters were observed between the distal metaphysis of WT and *EP1*$^{-/-}$ mice at 2-months of age. At 6-months of age, BV/TV in *EP1*$^{-/-}$ mice was not significantly different than at 2 months, while a significant decrease in BV/TV is observed in WT mice, relative to 2-months (−44%, p=0.0009), and aged matched *EP1*$^{-/-}$ mice (−34%, p=0.02). Moreover, at 1-year, the femur BV/TV remained significantly increased in *EP1*$^{-/-}$ mice, relative to WT (+37%, p=0.02). Both WT and *EP1*$^{-/-}$ mice had significant reductions in BV/TV during

aging; however, the extent of total bone loss was much greater in WT mice with a 173% loss in BV/TV from 2-months to 1-year, relative to a 65% loss in BV/TV in *EP1*$^{-/-}$ over the same time (Figure 1A & B). Tb.N was significantly decreased in WT mice at 1-year relative to 2-months (−122%), while a 62% reduction in Tb.N was observed in *EP1*$^{-/-}$ femurs. However, Tb.N remained significantly increased in *EP1*$^{-/-}$ mice, relative to WT at the same age, along with an increase in trabecular thickness at 6-months, and decreased trabecular spacing at 1-year-old (Figure 1C). In addition, microCT analysis of the mid-diaphyseal region showed a significant increase in polar moment of inertia in 1-year-old *EP1*$^{-/-}$ mice compared to age-matched WT mice (p=0.0004), indicating that EP1 has a significant impact on cortical bone geometry (Supplemental Figure 1).

Consistent with these findings, progressive loss of trabecular bone in the L4 vertebrae was observed in WT mice, with attenuation of bone loss in *EP1*$^{-/-}$ vertebrae (Figure 1D). BV/TV was significantly decreased in WT L4 vertebrae at 1-year (−60%, p=0.001), relative to *EP1*$^{-/-}$ (Figure 1E), while, Tb.N (−87%, p=0.002) and Tb.Th (−16%, p=0.03) were decreased and Tb.Sp (+28%, p=0.024) was increased at 6-months and 1-year, relative to *EP1*$^{-/-}$. No changes in L4 BV/TV, Tb. N., Tb.Th, and Tb.Sp were observed between *EP1*$^{-/-}$ mice between 2-months and 1-year (Figure 1F).

Elevated initial bone volume is protective against OVX-induced bone loss in EP1$^{-/-}$ mice

Osteoporosis is a condition characterized by progressive loss of bone density. Since *EP1*$^{-/-}$ mice show resistance to trabecular bone loss during aging, we further investigated whether *EP1*$^{-/-}$ mice may be also resistant to ovariectomy (OVX)-induced bone loss. Following surgery, serum β-estradiol levels of sham control group mice and OVX mice were determined. Both WT and *EP1*$^{-/-}$ OVX mice showed a significant decrease in β-estradiol levels compared to sham operated control mice (Supplemental Figure 2).

Following OVX the metaphyseal regions of the femora and vertebrae were examined by microCT. Consistent with the bone phenotype in 6-month old male mice, sham-operated female *EP1*$^{-/-}$ mice have significantly elevated femur BV/TV and Tb.Th., relative to sham operated WT females (Figure 2A–C), while no changes are observed between sham operated WT and *EP1*$^{-/-}$ L4 vertebrae (Figure 2D–F). In the femur metaphysis, BV/TV was significantly decreased in WT OVX relative to WT sham (−32%, p=0.035), and in *EP1*$^{-/-}$ OVX relative to *EP1*$^{-/-}$ sham (−37%, p=0.03) confirming that OVX accelerates trabecular bone loss (Figure 2B). However, BV/TV remains significantly increased in *EP1*$^{-/-}$ OVX mice, compared to WT OVX (+32%). Consistent with OVX-associated bone loss, WT OVX mice showed decreased femur trabecular number (−38%, p<0.05) and increased Tb.Sp (+26%, p<0.05) compared to WT sham mice. No changes in Tb.N or Tb.Th were observed between *EP1*$^{-/-}$ OVX and sham mice, however Tb.Sp was significantly increased (+17%, p<0.01). Consistent with an increase in starting BV/TV, *EP1*$^{-/-}$ OVX mice also have higher trabecular thickness (+25%) and lower trabecular spacing (−12%) compared to WT OVX mice (Figure 2C). In the metaphyseal region of L4 vertebrae, BV/TV is significantly decreased in both WT (−44%, p<0.01) and *EP1*$^{-/-}$ (−21%, p<0.05) mice. However, WT OVX mice have lower BV/TV (−24%, p=0.006), lower trabecular number and higher trabecular spacing compared to *EP1*$^{-/-}$ OVX mice. MicroCT analysis of femur cortical bone

demonstrated a significant decrease in polar moment of inertia in WT relative to *EP1*$^{-/-}$ in both sham control (−26%, $p<0.05$) and OVX (−35%, $p<0.05$) mice. In addition, Ct.Ar and Ct.Th were significantly decreased in WT mice in response to OVX, relative to sham; Ct.Th was also significantly decreased in WT OVX mice relative to *EP1*$^{-/-}$ OVX. No cortical bone changes were observed in *EP1*$^{-/-}$ mice following OVX (Supplemental Figure 1B).

EP1$^{-/-}$ mice are resistant to age and OVX-induced decrements in bone mechanical strength

Functionally, 3-point bending mechanical test results showed that max load at failure was significantly increased in *EP1*$^{-/-}$ femurs at 2-months (+19%), 6-months (+18%), and 1-year (+26%), relative to age-matched WT ($p<0.05$), while energy to max was significantly increased in *EP1*$^{-/-}$ at 6-months (+35%, $p<0.05$) and 1-year (+54%, $p<0.05$) (Figure 3A). *EP1*$^{-/-}$ L4 Max load was also significantly increased by 21% at 1-year, relative to WT, while energy to max was increased at 6-months and 1-year, relative to WT (Figure 3B).

OVX did not significantly decrease femur max load at failure in *EP1*$^{-/-}$, relative to respective sham controls ($p=0.08$), while WT OVX mice had a significant 15% decrease in max load, relative to sham ($p=0.01$). Max load was significantly increased in *EP1*$^{-/-}$ OVX, relative to WT OVX (+26%, $p<0.05$). In addition, OVX resulted in i) decreased energy to max in WT femurs but not in *EP1*$^{-/-}$ femurs compared to sham controls; and ii) increased energy to max in *EP1*$^{-/-}$ OVX femurs compared WT OVX (+26%, $p<0.05$) (Figure 3C). Moreover, compression tests performed on the L4 vertebrae revealed that *EP1*$^{-/-}$ mice are resistant to the changes in maximum load (WT: −58% relative to sham; *EP1*$^{-/-}$: −24% relative to sham) and energy to max (WT: −23% relative to sham, $p<0.05$; *EP1*$^{-/-}$: +7% relative to sham, $p=0.09$) caused by OVX (Figure 3D).

Bone formation but not resorption is increased in EP1$^{-/-}$ bones

In order to determine whether maintenance of bone mass during aging in *EP1*$^{-/-}$ mice was due to increased bone formation or decreased bone resorption, calcein labeling of new bone formation and TRAP staining of osteoclasts was conducted. MAR and BFR were significantly increased in *EP1*$^{-/-}$ mouse tibia (MAR: +27%, $p<0.05$)(Figure 4A) and calvaria (MAR: +50%, $p<0.05$) (Figure 4B) relative to WT. TRAP staining was performed on sections from the metaphyseal bone adjacent to the growth plate. Histomorphometric analysis of TRAP stained sections showed similar osteoclast number and resorption surface in the bones of EP1$^{-/-}$ and WT mice (Figure 4C). Collectively, these results suggest that the change in bone properties of the *EP1*$^{-/-}$ mice, especially the increased bone mineral density, is due to an increase in bone formation.

As osteoporosis is caused by the imbalance of bone formation and bone resorption, we examined the bone formation and resorption rates following OVX. Calcein double labeling demonstrated decreased MAR and BFR in both WT sham (MAR: −31%; BFR: −64%) and OVX (MAR: −19%; BFR: −73%) mice relative to *EP1*$^{-/-}$ sham and OVX mice, respectively ($p<0.05$). OVX resulted in a significant increase in both osteoclast number and resorption surface in WT and *EP1*$^{-/-}$ mice. No differences were observed between WT and *EP1*$^{-/-}$ in either sham or OVX mice (Figure 5B). Thus EP1 gene deletion does not alter the

bone resorption rate in sham or OVX mice, but does result in increased bone formation. These results suggest that the higher bone formation rate in *EP1*$^{-/-}$ mice compensates for the increased bone resorption caused by OVX and maintains trabecular bone mass. Furthermore, EP1 receptor gene deletion protects against the osteopenia and bone loss that result from aging.

EP1 is a negative regulator of bone formation

As *in vivo* studies show that *EP1*$^{-/-}$ mice have an increased bone formation rate and are resistant to age- and OVX-related bone loss, we examined whether EP1 antagonism in bone marrow stromal cells (BMSCs) could enhance osteogenic differentiation. Treatment of primary bone marrow cell cultures with the EP1 antagonist SD19220 enhanced bone nodule formation relative to vehicle treated cells after 12 days in culture. Alkaline Phosphatase staining was significantly increased 2.4-fold, relative to vehicle treated cells (p=0.009) (Figure 6A).

Discussion

In the present study we identified PGE2/EP1 signaling as a negative regulator of osteoblast differentiation and bone formation, and demonstrate for the first time that the EP1 receptor plays a negative role in regulation of postnatal bone homeostasis. We have previously demonstrated that *EP1*$^{-/-}$ mice exhibit accelerated fracture healing and that *EP1*$^{-/-}$ primary bone marrow progenitor cells differentiate into osteoblasts at an increased rate relative to WT cells, while osteoclastogenesis is not affected (17). Here we show that bones from *EP1*$^{-/-}$ mice have increased biomechanical strength, and increased bone volume when compared with WT mice. These differences are maintained or even amplified during aging, suggesting that *EP1*$^{-/-}$ mice are resistant to aging-induced bone loss due to an increase in bone formation rather than a decrease in bone resorption. *In vitro* experiments using an EP1 antagonist support that EP1 is a negative regulator of osteoblastogenesis. These findings show that in addition to regulating bone formation during injury and repair (17), activation of the EP1 receptor also has a critical role in the regulation of normal bone metabolism. No significant difference was found between WT and *EP1*$^{-/-}$ bone marrow progenitor cells in levels of the EP2 or EP4 receptors or of intracellular cAMP activity (17) suggesting that the bone phenotype in *EP1*$^{-/-}$ mice is not due to compensation by other EP receptors. These data, taken together with our previous findings of accelerated fracture repair in *EP1*$^{-/-}$ mice (17), and enhanced fracture healing with EP4 agonist treatment (2,4), highlight the complex nature of the effects of PGE2 on bone metabolism, which likely involves both stimulatory effects, through EP2 and EP4, and inhibitory effects mediated by EP1.

While showing that deletion of EP1 maintains femur bone volume fraction and trabecular bone parameters during aging, perhaps more importantly we have also demonstrated that increased initial BV/TV in *EP1*$^{-/-}$ is protective against OVX-induced bone loss. That is, while *EP1*$^{-/-}$ mice lose an approximately equal percentage of bone volume compared to WT, the relatively higher starting point results in bones that are stronger, and therefore less likely to fracture. Indeed, vertebral fractures are the most common osteoporotic fracture (18,19), and increase the risk for a subsequent vertebral or non-vertebral fracture (20–22).

Identification of EP1 loss of function as a mechanism to maintain vertebral bone density has profound implications for future osteoporosis treatments.

We have determined that EP1 modulates bone mass by regulating bone formation, but not bone resorption. This distinction is important since normal bone homeostasis requires an appropriate balance between bone formation and bone resorption, with un-coupling of these processes leading to pathologic bone changes including osteoporosis. The phenomenon of elevated bone formation with un-changed bone resorption in *EP1*$^{-/-}$ mice resulted in resistance to ovariectomy-induced bone loss. Our findings established that the increase in bone formation rate in *EP1*$^{-/-}$ mice was independent of estrogen status; bone formation was similarly increased in sham operated and OVX mice. These data suggest that inhibition of EP1 signaling may be a suitable target for the treatment of osteoporosis, although further studies are needed to elucidate the mechanism of EP1 effects on bone formation.

PGE2 has been identified as a central player in injury and repair through the regulation of murine stem and progenitor cell populations (23). PGE2 stimulation of EP2/4 stabilizes β-catenin, resulting in stem cell proliferation and differentiation (23,24). In contrast to EP2/4, which promote osteoblast differentiation (2,4), EP1 negatively regulates osteoblast differentiation, which may in turn, maintain the stem cell population, and act as a ‘brake’ to slow osteogenic differentiation of stem cells. While this hypothesis is speculative, it is well supported by many other findings. EP1 stimulates fibronectin expression, which helps to maintain osteoprogenitors in a more ‘stem-like’ state (25). Furthermore, EP1 activates AKT, leading to regulation of FoxO transcription factors, which maintain hematopoietic stem cells in a less mature state (26). Therefore, EP1 may be a key negative regulator in progression of stem cell differentiation, acting to maintain stem cells in a less differentiated state, as a mechanism to balance the physiological and pathological aspects of PGE2 signaling, however, further studies are necessary to clarify the role of EP1 in stem cell function.

Based on the clear role for EP1 in bone homeostasis and regeneration, further studies to define the downstream targets of EP1 will be critical to developing novel ways to treat osteoporosis and accelerate fracture repair. Specific agonists have been developed to target EP2 and EP4 receptors, demonstrating that these structurally related receptor subtypes are individually targetable. An issue with the EP2 and EP4 agonists was toxicity. Most pharmacologic agents are inhibitors, rather than stimulators of pathways, consistent with an approach that would be necessary for EP1-directed pharmacotherapy. Moreover, *EP1*$^{-/-}$ mice have normal lifespans, suggesting that inhibition of EP1 would be well tolerated. An alternative approach would be to block EP1 signaling through the inhibition of a downstream target. While these studies identify a critical role for EP1 in the negative regulation of bone formation, several limitations must be considered. In the present study, we use 12-month old mice to determine the effects of EP1 on age-related bone loss. However, given the maximum life-span for C57Bl/6J mice is approximately two years (27), the ‘aged’ mice in our study are comparable to sexually-mature adult humans, but do not necessarily reflect the changes in bone that are associated with elderly. Therefore, future studies to determine the effects of EP1 loss of function on bone maintenance in older months (>18 months) are necessary. Male mice were used for aging studies, while female mice were used for OVX experiments. The sexual dimorphism in bone strength and architecture

(28,29) precludes a direct comparison between OVX and aged animals. In addition, the potential effect of genetic drift between WT C57Bl/6J and *EP1*$^{-/-}$ mice must be considered, as purchased WT mice rather than littermate controls were used in this study. *EP1*$^{-/-}$ mice were generated on the C57Bl/6J background and were propagated through homozygous *EP1*$^{-/-}$ sibling breeding sets, a situation which can lead to natural genetic drift away from the original C57Bl/6J strain, which were purchased from Jackson laboratories and are less likely to experience genetic drift due to the Jackson Genetic Stability Program (30).

Taken together, we have identified the PGE2 receptor EP1 as a negative regulator of bone formation and suggest antagonism of PGE2/EP1 signaling as a potential therapeutic approach to inhibit age-related and OVX-induced bone loss and osteoporosis.

Supplementary Material

Refer to Web version on PubMed Central for supplementary material.

Acknowledgments

We would like to thank the Histology, Biochemistry and Molecular Imaging (HBMI) core for technical assistance with histology, and the Biomechanics and Multimodal Tissue Imaging (BMTI) Core for technical assistance with the biomechanical testing.

Supported by grants: This work was supported by NIH/NIAMS R01AR048681-06A1 (to RJO) and NSFC 81200255/H2501 (to MZ). The HBMI and BMTI cores are supported by NIH/NIAMS P30 AR061307 (to EMS).

References

1. Breyer RM, Bagdassarian CK, Myers SA, Breyer MD. Prostanoid receptors: subtypes and signaling. Annu Rev Pharmacol Toxicol. 2001; 41:661–90. [PubMed: 11264472]
2. Naik AA, Xie C, Zuscik MJ, Kingsley P, Schwarz EM, Awad H, Guldberg R, Drissi H, Puzas JE, Boyce B, Zhang X, O'Keefe RJ. Reduced COX-2 expression in aged mice is associated with impaired fracture healing. J Bone Miner Res. 2009; 24(2):251–64. [PubMed: 18847332]
3. Narumiya S, Sugimoto Y, Ushikubi F. Prostanoid receptors: structures, properties, and functions. Physiol Rev. 1999; 79(4):1193–226. [PubMed: 10508233]
4. Xie C, Liang B, Xue M, Lin AS, Loiselle A, Schwarz EM, Guldberg RE, O'Keefe RJ, Zhang X. Rescue of impaired fracture healing in COX-2−/− mice via activation of prostaglandin E2 receptor subtype 4. Am J Pathol. 2009; 175(2):772–85. [PubMed: 19628768]
5. Li TF, Zuscik MJ, Ionescu AM, Zhang X, Rosier RN, Schwarz EM, Drissi H, O'Keefe RJ. PGE2 inhibits chondrocyte differentiation through PKA and PKC signaling. Exp Cell Res. 2004; 300(1): 159–69. [PubMed: 15383323]
6. Li M, Healy DR, Li Y, Simmons HA, Crawford DT, Ke HZ, Pan LC, Brown TA, Thompson DD. Osteopenia and impaired fracture healing in aged EP4 receptor knockout mice. Bone. 2005; 37(1): 46–54. [PubMed: 15869929]
7. Machwate M, Harada S, Leu CT, Seedor G, Labelle M, Gallant M, Hutchins S, Lachance N, Sawyer N, Slipetz D, Metters KM, Rodan SB, Young R, Rodan GA. Prostaglandin receptor EP(4) mediates the bone anabolic effects of PGE(2). Mol Pharmacol. 2001; 60(1):36–41. [PubMed: 11408598]
8. Mano M, Arakawa T, Mano H, Nakagawa M, Kaneda T, Kaneko H, Yamada T, Miyata K, Kiyomura H, Kumegawa M, Hakeda Y. Prostaglandin E2 directly inhibits bone-resorbing activity of isolated mature osteoclasts mainly through the EP4 receptor. Calcif Tissue Int. 2000; 67(1):85–92. [PubMed: 10908419]
9. Miyaura C, Inada M, Suzawa T, Sugimoto Y, Ushikubi F, Ichikawa A, Narumiya S, Suda T. Impaired bone resorption to prostaglandin E2 in prostaglandin E receptor EP4-knockout mice. J Biol Chem. 2000; 275(26):19819–23. [PubMed: 10749873]

10. Yoshida K, Oida H, Kobayashi T, Maruyama T, Tanaka M, Katayama T, Yamaguchi K, Segi E, Tsuboyama T, Matsushita M, Ito K, Ito Y, Sugimoto Y, Ushikubi F, Ohuchida S, Kondo K, Nakamura T, Narumiya S. Stimulation of bone formation and prevention of bone loss by prostaglandin E EP4 receptor activation. Proc Natl Acad Sci U S A. 2002; 99 (7):4580–5. [PubMed: 11917107]
11. Suda M, Tanaka K, Natsui K, Usui T, Tanaka I, Fukushima M, Shigeno C, Konishi J, Narumiya S, Ichikawa A, Nakao N. Prostaglandin E receptor subtypes in mouse osteoblastic cell line. Endocrinology. 1996; 137(5):1698–705. [PubMed: 8612504]
12. Zhang M, Ho HC, Sheu TJ, Breyer MD, Flick LM, Jonason JH, Awad HA, Schwarz EM, O'Keefe RJ. EP1−/− mice have enhanced osteoblast differentiation and accelerated fracture repair. J Bone Miner Res. 2010
13. Zhen G, Kim YT, Li RC, Yocum J, Kapoor N, Langer J, Dobrowolski P, Maruyama T, Narumiya S, Dore S. PGE2 EP1 receptor exacerbated neurotoxicity in a mouse model of cerebral ischemia and Alzheimer's disease. Neurobiol Aging. 2012; 33(9):2215–9. [PubMed: 22015313]
14. Mohan S, Glushakov AV, Decurnou A, Narumiya S, Dore S. Contribution of PGE2 EP1 receptor in hemin-induced neurotoxicity. Front Mol Neurosci. 2013; 6:31. [PubMed: 24109429]
15. Guan Y, Zhang Y, Wu J, Qi Z, Yang G, Dou D, Gao Y, Chen L, Zhang X, Davis LS, Wei M, Fan X, Carmosino M, Hao C, Imig JD, Breyer RM, Breyer MD. Antihypertensive effects of selective prostaglandin E2 receptor subtype 1 targeting. J Clin Invest. 2007; 117(9):2496–505. [PubMed: 17710229]
16. Yan Y, Tang D, Chen M, Huang J, Xie R, Jonason JH, Tan X, Hou W, Reynolds D, Hsu W, Harris SE, Puzas JE, Awad H, O'Keefe RJ, Boyce BF, Chen D. Axin2 controls bone remodeling through the beta-catenin-BMP signaling pathway in adult mice. J Cell Sci. 2009; 122(Pt 19):3566–78. [PubMed: 19737815]
17. Zhang M, Ho HC, Sheu TJ, Breyer MD, Flick LM, Jonason JH, Awad HA, Schwarz EM, O'Keefe RJ. EP1(−/−) mice have enhanced osteoblast differentiation and accelerated fracture repair. J Bone Miner Res. 2011; 26(4):792–802. [PubMed: 20939055]
18. Riggs BL, Melton LJ 3rd. The worldwide problem of osteoporosis: insights afforded by epidemiology. Bone. 1995; 17(5 Suppl):505S–511S. [PubMed: 8573428]
19. Melton LJ 3rd, Kan SH, Frye MA, Wahner HW, O'Fallon WM, Riggs BL. Epidemiology of vertebral fractures in women. Am J Epidemiol. 1989; 129(5):1000–11. [PubMed: 2784934]
20. Black DM, Cummings SR, Karpf DB, Cauley JA, Thompson DE, Nevitt MC, Bauer DC, Genant HK, Haskell WL, Marcus R, Ott SM, Torner JC, Quandt SA, Reiss TF, Ensrud KE. Randomised trial of effect of alendronate on risk of fracture in women with existing vertebral fractures. Fracture Intervention Trial Research Group. Lancet. 1996; 348(9041):1535–41. [PubMed: 8950879]
21. Black DM, Palermo L, Nevitt MC, Genant HK, Epstein R, San Valentin R, Cummings SR. Comparison of methods for defining prevalent vertebral deformities: the Study of Osteoporotic Fractures. J Bone Miner Res. 1995; 10(6):890–902. [PubMed: 7572313]
22. Lindsay R, Silverman SL, Cooper C, Hanley DA, Barton I, Broy SB, Licata A, Benhamou L, Geusens P, Flowers K, Stracke H, Seeman E. Risk of new vertebral fracture in the year following a fracture. JAMA. 2001; 285(3):320–3. [PubMed: 11176842]
23. Goessling W, North TE, Loewer S, Lord AM, Lee S, Stoick-Cooper CL, Weidinger G, Puder M, Daley GQ, Moon RT, Zon LI. Genetic interaction of PGE2 and Wnt signaling regulates developmental specification of stem cells and regeneration. Cell. 2009; 136(6):1136–47. [PubMed: 19303855]
24. Fujino H, West KA, Regan JW. Phosphorylation of glycogen synthase kinase-3 and stimulation of T-cell factor signaling following activation of EP2 and EP4 prostanoid receptors by prostaglandin E2. J Biol Chem. 2002; 277(4):2614–9. [PubMed: 11706038]
25. Chen XD, Dusevich V, Feng JQ, Manolagas SC, Jilka RL. Extracellular matrix made by bone marrow cells facilitates expansion of marrow-derived mesenchymal progenitor cells and prevents their differentiation into osteoblasts. J Bone Miner Res. 2007; 2 (12):1943–56. [PubMed: 17680726]

26. Zhou P, Qian L, Chou T, Iadecola C. Neuroprotection by PGE2 receptor EP1 inhibition involves the PTEN/AKT pathway. Neurobiol Dis. 2008; 29(3):543–51. [PubMed: 18178094]

27. Yuan R, Tsaih SW, Petkova SB, Marin de Evsikova C, Xing S, Marion MA, Bogue MA, Mills KD, Peters LL, Bult CJ, Rosen CJ, Sundberg JP, Harrison DE, Churchill GA, Paigen B. Aging in inbred strains of mice: study design and interim report on median lifespans and circulating IGF1 levels. Aging Cell. 2009; 8(3):277–87. [PubMed: 19627267]

28. Callewaert F, Venken K, Kopchick JJ, Torcasio A, van Lenthe GH, Boonen S, Vanderschueren D. Sexual dimorphism in cortical bone size and strength but not density is determined by independent and time-specific actions of sex steroids and IGF-1: evidence from pubertal mouse models. J Bone Miner Res. 2010; 25(3):617–26. [PubMed: 19888832]

29. Seeman E. Clinical review 137: Sexual dimorphism in skeletal size, density, and strength. J Clin Endocrinol Metab. 2001; 86(10):4576–84. [PubMed: 11600506]

30. Taft RA, Davisson M, Wiles MV. Know thy mouse. Trends Genet. 2006; 22(12):649–53. [PubMed: 17007958]

Highlights

- $EP1^{-/-}$ mice have significantly increased BV/TV, relative to WT during aging
- $EP1^{-/-}$ mice are protected against decrements in mechanical properties after OVX
- Bone formation is enhanced in $EP1^{-/-}$ mice, relative to WT
- No change in osteoclast number is observed between WT and $EP1^{-/-}$ mice

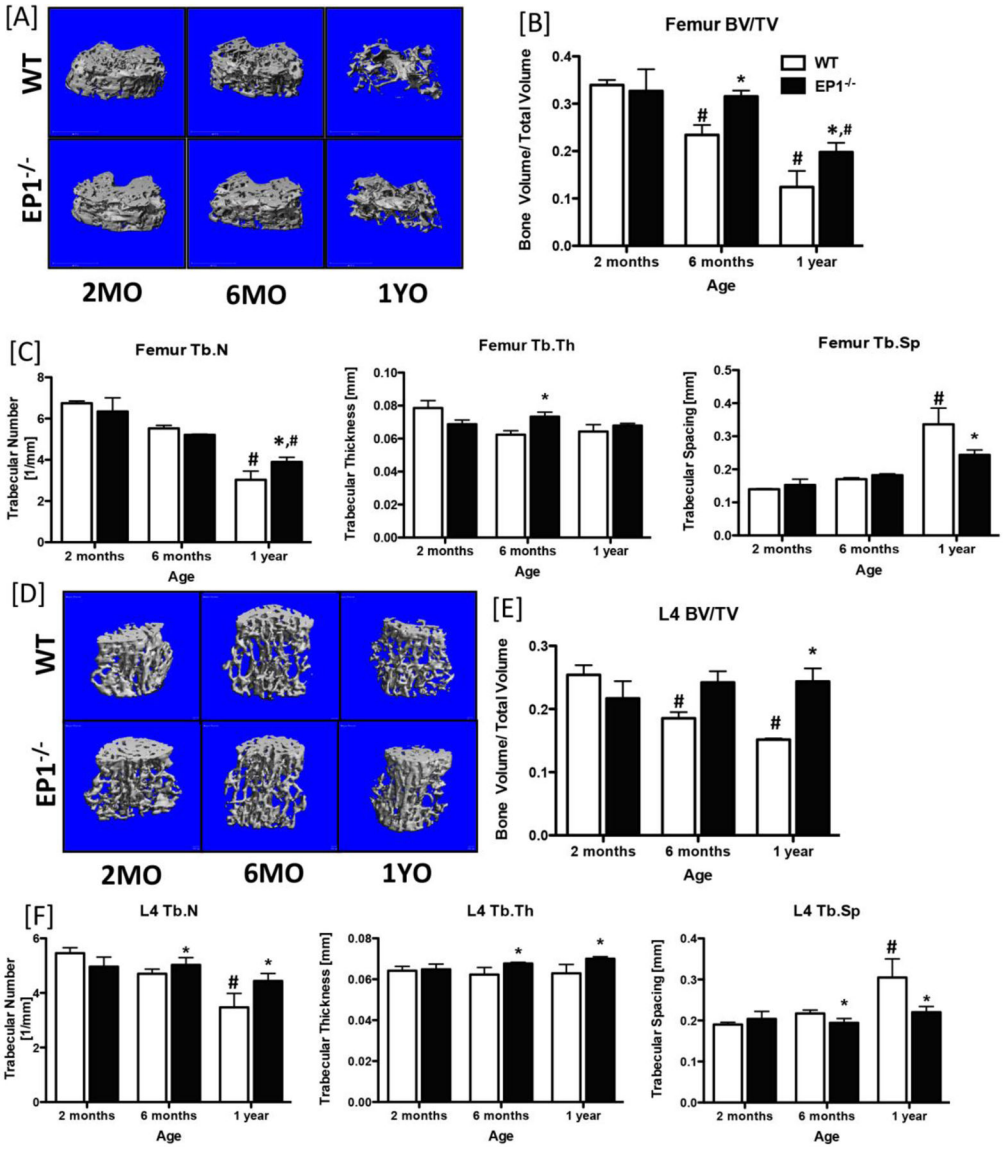

Figure 1. Loss of EP1 is protective against age-induced bone loss

Three-dimensional microCT reconstructions of the metaphyseal femur [A] and L4 vertebrae [D] of WT and EP1$^{-/-}$ mice at 2-months, 6-months and 1-year of age. [B & E] Bone volume/total volume; [C & F] trabecular number, trabecular spacing, and trabecular thickness quantification of the femur and L4 vertebrae, respectively. N = 5 per group. Statistical analysis was performed using 2-way ANOVA followed by Dunnett's test. (*) = $p < 0.05$ v.s. age-matched WT, (#) = $p < 0.05$ v.s. respective genotype at 2-months.

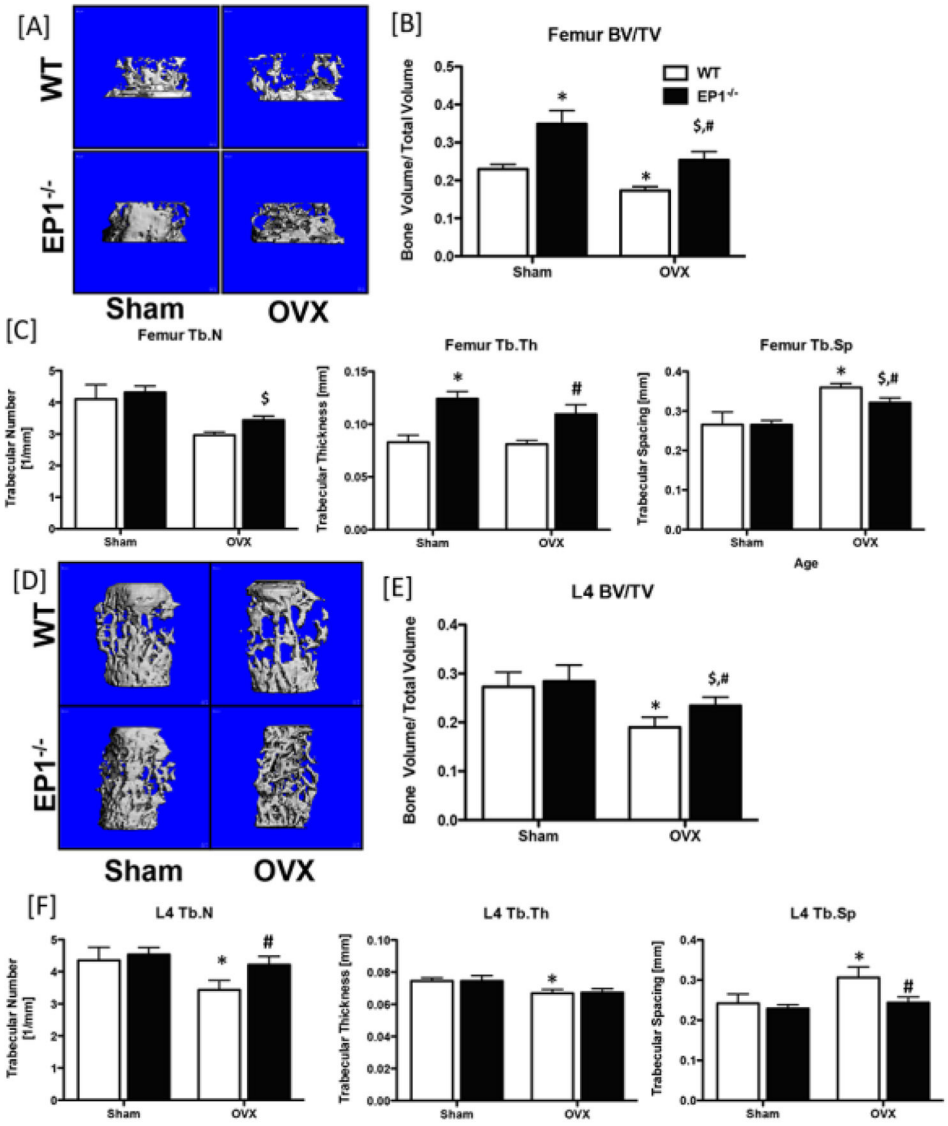

Figure 2. Loss of EP1 protects against ovariectomy-induced bone loss

Sham or OVX surgeries were performed on 4-month-old *EP1*$^{-/-}$ and WT mice. Trabecular bone regions in the metaphyseal femur [A] and the vertebral body [D] were examined. [B & E] Bone volume/total volume; [C & F] trabecular number, trabecular spacing, and trabecular thickness quantification of the femur and L4 vertebrae, respectively. N = 5 per group. Statistical analysis was performed using 2-way ANOVA followed by Dunnett's test. (*) = $p < 0.05$ v.s. WT sham, ($) = $p<0.05$ vs KO Sham, (#) = $p < 0.05$ v.s. WT OVX.

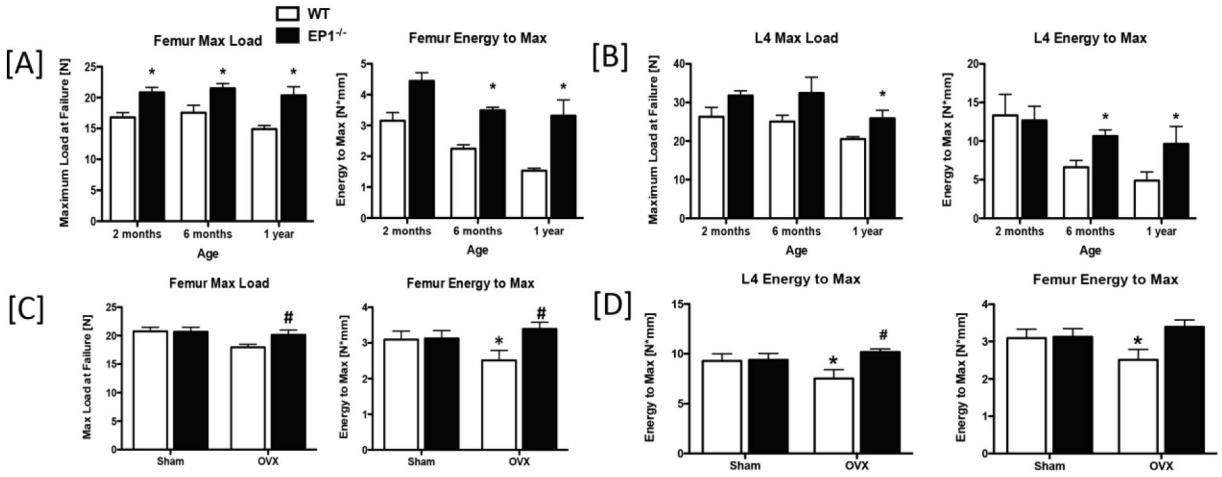

Figure 3. *EP1*$^{-/-}$ mice have enhanced bone biomechanical properties

[A] Maximum load at failure, and energy to max from 3-point bending analysis of WT and *EP1*$^{-/-}$ femurs harvested from 2-month, 6-month, and 1-year-old mice. [B] Max load at failure, and energy to max of L4 vertebrae of WT and *EP1*$^{-/-}$ mice at 2-months, 6-months, and 1-year of age, which underwent compression testing. [C] Maximum load at failure, and energy to max from 3-point bending analysis of WT and *EP1*$^{-/-}$ femurs harvested from 8-weeks after OVX. [D] Max load at failure, and energy to max of L4 vertebrae of WT and *EP1*$^{-/-}$ mice 8-weeks after OVX. N = 5 per group. Statistical analysis was performed using 2-way ANOVA followed by Dunnett's test. (*) = $p < 0.05$ v.s. age-matched WT.

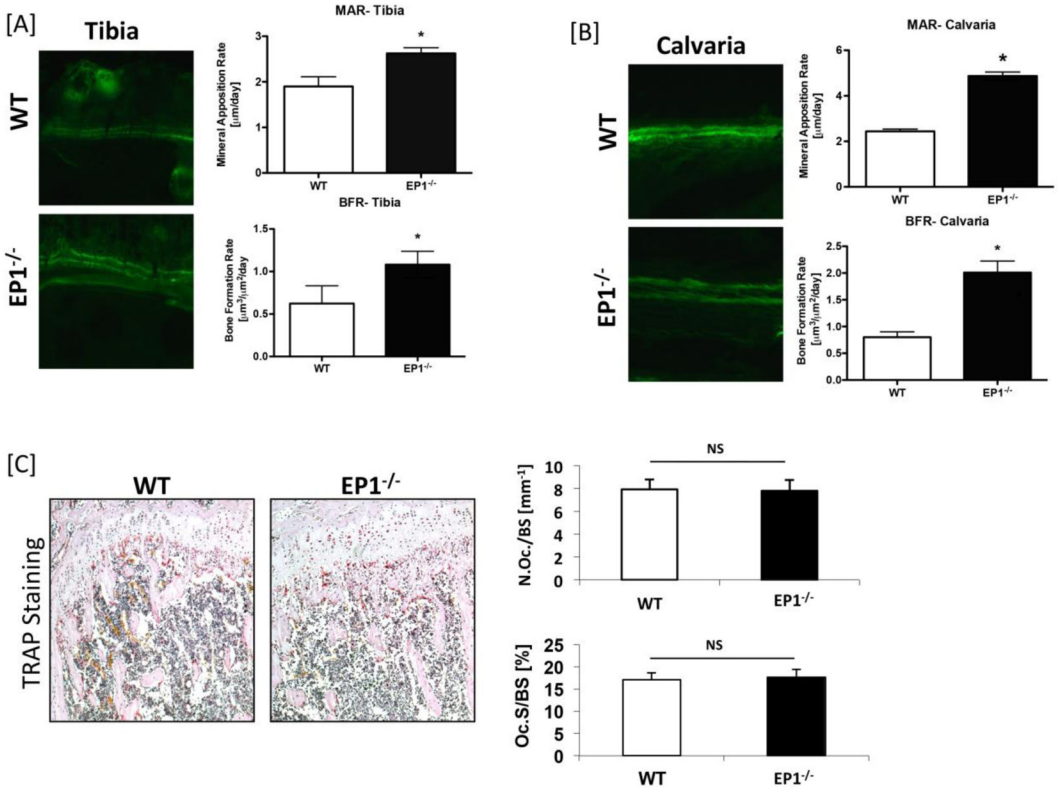

Figure 4. *EP1*$^{-/-}$ mice show increased bone formation and normal bone resorption

Calcein labeling was performed on 10 week-old *EP1*$^{-/-}$ and WT mice. Sections of [A] Tibia and [B] Calvaria were examined by fluorescence microscopy and mineral apposition rates (MAR) and bone formation rates (BFR) were quantified. [C] Femurs from 2 month-old *EP1*$^{-/-}$ and WT mice underwent TRAP staining to identify TRAP+ osteoclasts; Osteoclast number/bone surface (Oc.N./BS) and osteoclast surface/bone surface (Oc.S./BS) were quantified. Statistical comparisons were performed using Student's t-test. 5 mice, 3 levels per mouse, were tested in each group, N = 5. (*) = $p < 0.05$ v.s. WT. Not significant is denoted as "NS".

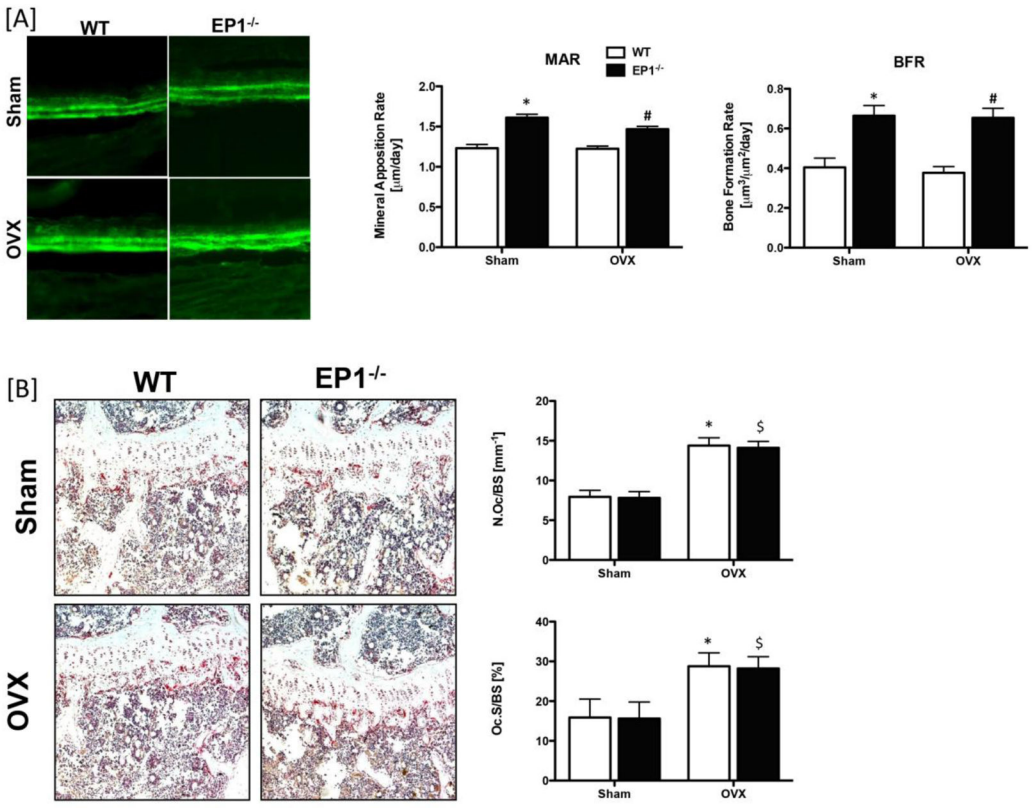

Figure 5. Ovariectomy does not affect bone formation rate in *EP1*$^{-/-}$ mice

[A] Calcein labeling was performed on sham or OVX operated WT and EP1$^{-/-}$ mice. Tibia were examined by fluorescence microscopy and mineral apposition rates (MAR) and bone formation rates (BFR) were quantified. [B] Femur and tibia were harvested for TRAP staining. Osteoclast numbers/bone surface (Oc.N/BS) and resorption surface (Oc.S/BS) were quantified. Statistical analysis was performed using 2-way ANOVA followed by Dunnett's test, N = 5 mice per group were examined. (*) = $p < 0.05$ v.s. WT sham, ($) = $p < 0.05$ v.s. KO sham, (#) = $p < 0.05$ v.s. WT OVX.

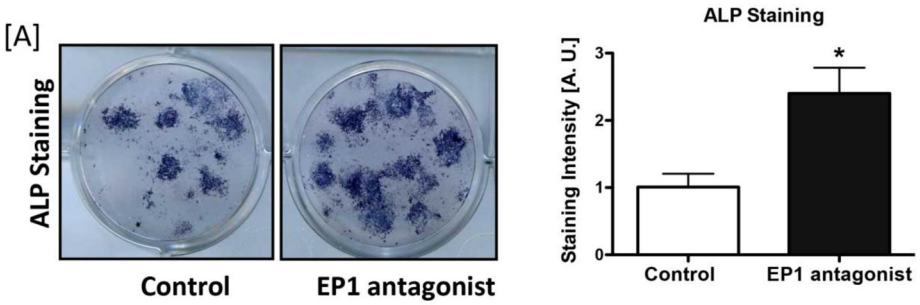

Figure 6. EP1 is a negative regulator of bone formation

[A] WT Bone marrow progenitor cells were treated with 10 μM of the EP1 antagonist SC19220 for 5 days in osteogenic media. Cells were then stained for Alkaline Phosphatase.